THERMAL CYCLING STABILITY OF FLY ASH BASED GEOPOLYMER MORTARS

F. Colangelo[a], R. Cioffi[a], G. Roviello[a], I. Capasso[b], D. Caputo[b], P. Aprea[b], B. Liguori[b], C. Ferone[*a]

[a] Materials Science and Engineering Research Group MASERG, Dipartimento di Ingegneria, Università Parthenope, Centro Direzionale Is. C4, Napoli, Italy

[b] ACLabs Laboratori di Chimica Applicata, Dipartimento di Ingegneria Chimica, dei Materiali e della Produzione Industriale, Università di Napoli Federico II, P.le Tecchio 80, Napoli, Italy.

[*]Corresponding author: Claudio Ferone – email: claudio.ferone@uniparthenope.it – Centro Direzionale, Is. C4 – 80143 Napoli (Italy) – Phone N. +390815476713

Abstract

In this paper fly ash based geopolymer mortars have been prepared and their thermal behavior evaluated in order to assess the suitability of fly ash based alkali-activated binders for thermal energy storage in solar thermal plants. Different parameters, such as binder/aggregate ratio, percentage of fly ash replaced by slag, temperature and curing time, have been changed and optimized using the Design Of Experiments (DOE) approach. In order to estimate the thermal cycling stability of geopolymeric mortars at elevated temperatures, mechanical strength and weight loss of each sample subjected to different thermal cycles in the temperature range 150-550°C were evaluated. Finally,

thermal conductivity of some of the mixtures, selected on basis of the thermal stability test results, have been measured.

Fly ash based geopolymeric mortars remained stable after each thermal treatment and specimens treated at elevated temperatures retained acceptable compressive strength. The thermal stability was preserved also after repeated thermal cycles, proving that fly ash based geopolymers are suitable materials for thermal energy storage concretes.

Keywords: fly ash; geopolymer mortar; energy storage materials; thermal stability.

Introduction

Geopolymers are hydraulic binders produced from the reaction of natural or synthetic silico-aluminate powders, often generated from industrial waste [1], in an alkaline environment (silicate solution and sodium hydroxide and / or potassium). Recently, geopolymers have been proposed in different applications, in the military and aeronautical field, as high-tech ceramic materials, thermal insulators, fire-resistant materials, protective coatings, refractory adhesives and hybrids inorganic-organic composites [2-7].

Geopolymers have been proposed also as a viable alternative to cement in concrete. In fact, in order to reduce the environmental impact of standard OPC concrete, the most employed material in the world after water, two routes can be pursued: 1) the use of eco-sustainable aggregates [8 – 12]; 2) the use of eco-sustainable binders, such as geopolymers [13 - 20]. A third option, the most environmentally friendly, is a combination of the first two.

Geopolymers also provide an opportunity to convert a variety of waste streams into useful by-products [20]. These materials show excellent thermal resistance (T > 1200 °C), even for long exposures to high temperatures [21, 22]. Fly ash and blast furnace slag based concretes have been tested for thermal resistance up to 800 °C, evidencing a decay of the properties at temperatures higher than 600 °C [23, 24]. Moreover, thermal resistance can be further improved using different strategies [18, 25 - 28].

Fly ash and other natural and industrial by-products, currently disposed of as waste, have been researched as potential reuse opportunities [29 - 34] especially as a supplementary cementitious material in cement [35] and as a feedstock for geopolymers [36 - 42]. A recent paper concerning the numerical modeling of concretes for thermal energy storage (TES) [43] showed promising results on the use of fly ash based geopolymer concrete for this purpose.

In this paper, fly ash based geopolymeric mortars were prepared and characterized in order to evaluate their thermal behaviour under repeated thermal cycles. Low calcium fly ash and blast furnace slag were employed as aluminosilicate source and some different process parameters were changed, such as the binder/aggregate ratio, the percentage of fly ash replaced by slag, the temperature and the time of curing. One of the goals was to assess the suitability of fly ash based geopolymer binders for thermal energy storage (TES) in solar thermal plants.

This application requires not only resistance at high temperature, but also to prolonged thermal cycles [44]. Thus, the thermal behavior was assessed by monitoring physical-mechanical properties before and after thermal cycles, this approach being more representative of the actual operative conditions respect to thermal treatments constituted by a heating ramp, an isothermal step and a slow cooling.

In the present paper, mechanical strength, ultrasonic pulse velocity, weight loss and microstructural features of each mortar subjected to different step thermal cycles in the temperature range 150-550°C, were evaluated. Applied testing conditions are much harsher than actual operative situation, where heating and cooling rates are slower. Thermal conductivity of selected mortars, based on the results of thermal tests, was also measured in order to assess the effective application of these materials.

Materials and methods

Geopolymeric mortars were prepared starting from fly ash with low calcium content (Class F – ASTM C 618) deriving from the combustion of coal. Fly ash (FA), supplied by ENEL (Brindisi, Italy) did not meet standard specifications EN 450 (EN 450-1:2012) for use in concrete thus potentially showing a lower pozzolanic activity [45]. Composition of FA is reported in table 1. The alkaline solution was prepared mixing a sodium silicate solution (SS) (Na_2O 8.15 wt.%, SiO_2 27.40wt.%) provided by Prochin Italia S.r.L. (Marcianise (CE)) with 10 M sodium hydroxide solution (N) prepared starting from NaOH in pellets (NaOH 98wt.%, J.T. Baker, “Baker analyzed”) and bi-distilled water. The weight ratio SS/N/FA was 1: 1: 3, based on previous studies results [45]. The sand used as aggregate is a standard (UNI-EN 196-1:2016) siliceous sand.
In some of the mixtures, ground granulated blast furnace slag (GGBFS), supplied by Italcementi (Brindisi, Italy) whose composition is reported in table 1, was added in replacement of fly ash.
The organization of the experiments was conducted using the Design Of Experiments (DOE) approach, considering a system of four factors that can change on three levels. DOE technique enables designers to control simultaneously the individual and interactive effects of many factors that could affect the output results for any design. The space of the experiments was explored using a fractional factorial design (an

orthogonal array (L9) has been used [46]). The binder/aggregate ratio (B/A), the percentage of FA substituted by GGBFS (A), the temperature (T) and time of curing (t) were chosen as the active factors. The resulting matrix of experiments, containing the different levels used for each parameter, is shown in Table 2.

Solid raw materials, fly ash, sand and, eventually, blast furnace slag, were mixed and dry homogenized in a Hobart mixer for 5 minutes, then the alkaline solution was added to the dry mixture and mixed for further 10 minutes. The binder/aggregate ratios chosen were 1:0.75, 1:1 and 1:2. The mixtures were subsequently cast in cubic Plexiglas molds (5x5x5 cm), covered by a PVC film to prevent evaporation and cured at 25, 40 or 60°C for 24, 48 and 168 hours. After this period of curing, the specimens were removed from the molds and stored at room temperature. After 28 days, three specimens for each mixture were tested for compressive strength using a compressive strength test machine Controls (mod. MCC8) with a load cell of 300 kN.

The remaining specimens were subjected to thermal cycles as follows: three specimens for each mixture underwent a thermal treatment in air at five different temperatures, i.e. 150, 250, 350, 450 and 550°C, using a Nabertherm HTC 03/15 oven. These temperatures were chosen to evaluate the behaviour of the mixtures at thermal levels similar or slightly higher than those experienced in a TES system [43]. The thermal treatment was performed according to the following procedure: each specimen, put in the oven at the specified temperature, was removed after 30 min, left on a refractory brick at room temperature for 5 minutes and subsequently its mass was measured. A Mettler Toledo XS105 Dual Range microbalance with an accuracy of ± 0.1 mg was used. This procedure was repeated 8 times, for a total of 4 h of thermal treatment. In this way, it was possible to evaluate the thermal shock resistance of the material inasmuch as each specimen was subjected to a series of nine rapid heating and cooling cycles. Furthermore, at the end of each series of thermal treatments, the compressive strength of

the specimens was measured. The apparent density of the specimens before and after thermal treatment was calculated by dividing the mass by the geometrical volume. Mechanical properties of mortars were estimated also by ultrasonic non-destructive testing. The ultrasonic measurements were performed weekly during the 28 days of curing on each mortar using an ultrasonic pulse velocity (UPV) tester Matest mod. C368, in order to determine the time of propagation of pulses within the considered materials at different moments of curing.

The UPV test was used as a non-destructive technique to evaluate qualitatively the stiffness evolution of the mixtures, which is primarily influenced by the amount of percolated solids, the porosity and the inner cracks of the paste. Recently, an alternative technique, i.e. Acoustic Emission Technique, has been used for the same purpose [47]. Usually, the UPV results are correlated to dynamic elastic modulus of concrete. No theoretical correlation exists between UPV and strength, so ultrasonic testing is useful if intended as complementary tool. The equipment used for the testing is a UPV tester with microprocessor compliant with BS1881:203, EN 12504 part 4, ASTM C597, EN/ISO 8047.

Room temperature thermal conductivity was measured by using a Unitherm 2022 instrument, by Anter Corporation. This measurement was carried out on mortar discs (d=5cm; H=1.25cm) according to the guarded heat flow meter test method (ASTM E1530). Four specimens were employed for each mortar.

Furthermore, geopolymer samples were subjected to SEM observation to evaluate microstructural features. Freshly fractured surfaces were coated with gold and observed by a FEI Quanta 200 FEG microscope.

Results and discussion

In table 3 the compressive strength (R_c) after 28 days of curing, the variations of mass (**Δm**), density (**Δρ**) and mechanical strength (**ΔRc**) of each sample after the 150°C-thermal treatment are reported.

Compressive strength of untreated samples was rather low compared to that obtainable with a common FA based geopolymer [48], likely caused by the quality of the FA employed in this work [49]. Nevertheless, the highest values are comparable to those of a normal-strength concrete, according to UNI EN 206 (2006). Furthermore, high compressive strength is not required for concrete used for thermal applications [48].

All the specimens showed: a good dimensional stability (ΔV <0.5%, values not reported), a mass loss lower than 5%, and a decrease in mechanical properties. Even if a general decay in mechanical properties was detected, data appeared more scattered than mass and volume variation.

In order to select the most reliable mortars from a thermomechanical point of view, an "objective function" OF, which took into account the mechanical properties of each sample and their variation after the thermal treatment, was defined as follows:

$$OF = \frac{R_i^b}{\overline{R^b}} + 2\frac{\Delta R^i}{\overline{R^a}}$$

where:

R_i^b = compressive strength of the mixture i before thermal treatment;

$\overline{R^b}$ = average compressive strength before thermal treatment

ΔR^i= compressive strength variation of the mixture i after thermal treatment

$\overline{R^a}$ = average compressive strength after thermal treatment.

The first addendum of such function depends on the initial strength of the sample, while the second one takes into account the strength variation after the thermal treatment. Globally, the function increases with the initial strength and decreases if the thermal

treatment induces a loss of strength, helping to identify the best mixtures. In order to take into account the higher importance of compressive strength variation with respect to its initial value, an amplification factor (equal to 2) was introduced into the formula. The histogram shows the value of the function for each mixture, clearly revealing that the mixtures 3, 6 and 9 have the best performance (Figure 1).

The response of the process to each parameter has been evaluated by calculating, for each factor, the means of every OF of the experiments conducted with that factor at each level. Figure 2 reports such data in a graphical form: it can be seen that the temperature has a strong influence on the material performances. The additive also influence the system, but in a negative way: the higher the additive content, the lower the OF. Curing time and B/A do not substantially influence the OF.

Based on the above results, mortars 3, 6 and 9 were selected for the subsequent heat treatments up to 550°C.

Mass losses increased with time due to dehydration processes, which took place mainly during the first hour of treatment and reached equilibrium a few minutes later (Figure 3). Geopolymers, that are mainly silicoaluminates, show a gradual loss of the OH groups during heating, which produces microporosity within the matrix [50]. All the samples underwent a significant decrease in density with the thermal treatment (Table 4). Considering $\Delta\rho$, the three samples showed noticeably different thermal behavior. A significant decrease around 7% was reached at different temperatures: 550°C for mortar 3, 450°C for mortar 6 and 350°C for mortar 9. This behaviour is related to the B/A ratio, which increases with this same order (3-6-9).

Comparing the average values of mechanical properties after each thermal treatment for temperatures from 250 to 550°C (Table 4 - fifth row), it appears evident that mortars 3 and 6 show a higher mechanical stability than mortar 9. This may in part be due to the

lower amount of aggregate present in the mixture 9, confirming the results of density variation.

In Figure 4 the average values of UPV (ultrasonic pulse velocity) obtained for each kind of mortar at different curing times are reported. The UPV in the mortars 3 and 6 increased with curing from 7 to 28 days, confirming that the structure becomes more rigid with curing [51]. Mortar 9 did not show a definite trend, as UPV values did not significantly change, and had the largest variability during measurements. Overall, for all three mortars, the variation in UPV values between 7 and 28 days was small and the UPV can be deemed to be practically constant. Therefore, as the three mortars were cured at 60°C, we can deduce that curing at this temperature likely results in an almost complete hardening of the samples after 7 days.

The measurements of the UPV values within each specimen were carried out also after each thermal treatment, in order to control microstructure homogeneity of the geopolymeric mortars.

UPV decreased with increasing temperatures for each mortar (Figure 5). In fact, water content within the mortar is still high at low temperature, so the propagation velocity of ultrasonic pulses is higher. However, the propagation becomes slower when water is replaced by air during the continued drying [52].

Mortar 3 showed the lowest values of UPV, confirming that it is more porous than the other samples. In fact, as reported in the literature [53, 54], the speed of sound in a ceramic material decreases approximately proportionally with an increase in porosity. This had a similar effect on Young's modulus and Poisson's ratio, both decreasing as the porosity of the sample increased [54]. A further confirmation is provided by the measurement of mechanical strengths, where mortar 3 showed the lowest value of compressive strength compared to mortars 6 and 9 (Table 3).

The thermal characterization was improved with the measurement of the thermal conductivity (Table 5). The measured values are consistent with those reported in the literature [55] and lower than those reported in [43]. Slight differences in composition and curing conditions can justify this dissimilarity. Regardless, thermal conductivity could be improved for the specific application (TES) by using for example high density and high conductivity aggregates.

Additional information was collected by microstructure characterization of each geopolymeric mortar. SEM micrographs at 1000X of freshly fractured surfaces of samples 3, 6 and 9 cured at 60°C and thermally treated at 150°C and 550°C are reported in Figure 6. Specimens cured at 60°C (figures 6a, d and g) have a microstructure characterized by a rather homogeneous geopolymer matrix embedding the sand particles. Worth noting is the excellent adhesion between the matrix and the sand particles for the mixtures 6 and 9 (figures 6d and 6g). In the case of sample 6, the adhesion is excellent even with sand particles of higher size (figure 6d) which represent the hardest situation in terms of Interfacial Transition Zone (ITZ) formation [4]. With thermal treatment at 150°C the matrix becomes porous and fractures owing to the water evaporation, especially in the case of samples 9 and 3, respectively (figures 6h and 6b). In the case of sample 3, the situation is even worse, because the sand particles appear detached from the matrix and the ITZ is clearly visible. The thermal treatment at 550°C confirms the worsening of the microstructural features of the samples. However, unlike what happens in the specimen 3 where the ITZ is evident, specimens 6 and 9 are characterized only by a deterioration of the matrix. The latter remains in any case well adherent to the sand particles, especially for specimen 9 (figure 6i). These considerations are in good agreement with the composition of the specimens and with the R_c, UPV and mass loss results. In fact, the strength and the UPV values of the samples decrease with increasing temperature, in particular for specimen 3 which has

the lowest binder/aggregate ratio. The minor deterioration of the matrix in sample 6 might be due to the absence of slag in this sample and the consequent lower percentage of hydrated phases, as confirmed also by the low mass loss of the sample.

Conclusions and future developments

This paper mainly focuses on the weight change, strength loss and UPV variation of different fly ash based geopolymer mortars, after repeated thermal cycles, in order to assess the suitability of these materials as thermal energy storage system. The results are positive as the produced geopolymeric mortars did not show phenomena of spalling or fracturing or other kinds of visible deterioration in exposure conditions much harsher than those experienced in actual operative conditions. The strength loss is evident, particularly at the higher temperatures, but does not hinder the use of this material in TES systems as residual strength sufficiently high was attained after the thermal cycles. In addition, a first evaluation of the dimensional stability gave promising results. According to the obtained results, the best candidate to be used as TES material is the mixture 6, containing no GGBFS, cured at 60°C and with a binder to aggregate ratio of 1 : 1. In fact, good strength and UPV were observed, the mixture maximizes the percentage of fly ash, shows a low mass loss and a consequent good dimensional stability.

An optimization of the system, in terms of the thermal properties, is needed, as a first measurement of thermal conductivity provided values which are too low for the specific application. For example, the addition of additives or fillers, such as graphite powder or metal fibres, or the replacement of the traditional aggregates with denser ones will be evaluated.

Acknowledgements

This research study has been funded by the University of Napoli “Parthenope” with a grant within the call “Support for Individual Research for the 2015-17 Period” issued by Rectoral Decree no. 727/2015. The support is gratefully acknowledged.

References

1 Davidovits, J. (1993). “Geopolymer cements to minimise carbon-dioxide greenhouse-warming.” *Ceramic Transactions*, 37, 165-182.

2 Kriven W.M. (2017). “Geopolymer-Based Composites.” *Reference Module in Materials Science and Materials Engineering*, Current as of 29 April 2017

3 Menna, C., Asprone, D., Ferone, C., Colangelo, F., Balsamo, A., Prota, A., Cioffi, R., Manfredi, G. (2013). “Use of geopolymers for composite external reinforcement of RC members.” *Compos. Part B-Eng.* 45, 1667-1676.

4 Colangelo, F., Roviello, G., Ricciotti, L., Ferone, C., Cioffi, R. (2013). “Preparation and characterization of new geopolymer-epoxy resin hybrid mortars.” *Materials*, 6(7), 2989-3006.

5 Roviello, G., Ricciotti, L., Ferone, C., Colangelo, F., Cioffi, R., Tarallo, O. (2013) “Synthesis and characterization of novel epoxy geopolymer hybrid composites.” *Materials*, 6 (9), 3943-3962.

6 Roviello, G., Ricciotti, L., Ferone, C., Colangelo, F., Tarallo, O. (2015). “Fire resistant melamine based organic-geopolymer hybrid composites.” *Cement Concrete Comp*. 59, 89-99.

7 Masi G., Rickard W.D.A., Bignozzi M. C., van Riessen A. (2015). “The effect of organic and inorganic fibres on the mechanical and thermal properties of aluminate activated geopolymers.” *Compos. Part B-Eng*. 76, 218-228

8 Singh N., Hui D., Singh R., Ahuja I.P.S., Feo L., Fraternali F. (2017) “Recycling of plastic solid waste: A state of art review and future applications.” *Compos. Part B-Eng.* 115, 409-422.

9 Colangelo, F., Messina, F., Di Palma, L., Cioffi, R. (2017) “Recycling of non-metallic automotive shredder residues and coal fly-ash in cold-bonded aggregates for sustainable concrete.” *Compos. Part B-Eng.* 116, 46-52.

10 Colangelo, F., Cioffi, R. (2017) “Mechanical properties and durability of mortar containing fine fraction of demolition wastes produced by selective demolition in South Italy.” *Compos. Part B-Eng.*, 115, 43-50.

11 Dembovska, L., Bajare, D., Ducman, V., Korat, L., Bumanis, G. (2017) “The use of different by-products in the production of lightweight alkali activated building materials.” *Construction and Building Materials*, 135, 315-322.

12 Colangelo, F., Cioffi, R., Liguori, B., Iucolano, F. (2016) “Recycled polyolefins waste as aggregates for lightweight concrete.” *Compos. Part B-Eng.*, 106, 234-241.

13 Palomo, A., Grutzeck, M.W., Blanco, M.T. (1999). “Alkali-activated fly ashes: a cement for the future.” *Cement Concrete Res*., 29, 1323-1329.

14 Duxson, P., Provis, J.L., Lukey, G.C., van Deventer, J.S.J. (2007). “The Role of Inorganic Polymer Technology in the Development of Green Concrete.” *Cement Concrete Res.*, 37(12), 1590-1597.

15 Andini, S., Cioffi, R., Colangelo, F., Grieco, T., Montagnaro, F., Santoro, L. (2008). “Coal fly ash as raw material for the manufacture of geopolymer-based products.” *Waste Manage*., 28, 416-423.

16 Ferone, C., Colangelo, F., Roviello, G., Asprone, D., Menna, C., Balsamo, A., Prota, Manfredi, G. (2013). “Application-oriented chemical optimization of a metakaolin based geopolymer.” *Materials*, 6(5), 1920-1939.

17 McLellan, B.C., Williams, R.P., van Riessen, A., Lay, J., Corder, G.D. (2011). "Costs and carbon emissions for geopolymer pastes in comparison to ordinary Portland cement." *J. Clean. Prod.* 19, 1080-1090.

18 Balcikanli, M., Ozbay, E. (2016) "Optimum design of alkali activated slag concretes for the low oxygen/chloride ion permeability and thermal conductivity." *Compos. Part B-Eng.*, 91, 243-256

19 Görhan, G., Aslaner, R., Şinik, O. (2016). "The effect of curing on the properties of metakaolin and fly ash-based geopolymer paste." *Compos. Part B-Eng.*, 97, 329-335.

20 Singh, B., Ishwarya, G., Gupta, M., & Bhattacharyya, S. K. (2015). "Geopolymer concrete: A review of some recent developments". *Construction and Building Materials*, 85, 78-90.

21 Zhang, H. Y., Kodur, V., Wu, B., Cao, L., & Wang, F. (2016). "Thermal behavior and mechanical properties of geopolymer mortar after exposure to elevated temperatures." *Construction and Building Materials*, 109, 17-24.

22 Kong, D. L., Sanjayan, J. G., & Sagoe-Crentsil, K. (2007). "Comparative performance of geopolymers made with metakaolin and fly ash after exposure to elevated temperatures." *Cement and Concrete Research*, 37(12), 1583-1589.

23 Ren, W., Xu, J., Bai, E. (2015). "Strength and Ultrasonic Characteristics of Alkali-Activated Fly Ash-Slag Geopolymer Concrete after Exposure to Elevated Temperatures." *Journal of Materials in Civil Engineering*, 10.1061/(ASCE)MT.1943-5533.0001406, 040015124.

24 Kürklü G. (2016) "The effect of high temperature on the design of blast furnace slag and coarse fly ash-based geopolymer mortar." *Compos. Part B-Eng.*, 92, 9-18

25 Bernal S. A., Bejarano J., Garzón C., de Gutiérrez R. M., Delvasto S., Rodríguez E. D. (2012) "Performance of refractory aluminosilicate particle/fiber-reinforced geopolymer composites." *Compos. Part B-Eng.*, 43, 4, 1919-1928

26 Rickard, W. D., Borstel, C. D., Van Riessen, A. (2013). “The effect of pre-treatment on the thermal performance of fly ash geopolymers.” *Thermochimica Acta*, 573, 130-137.

27 Vickers, L., Rickard, W. D., van Riessen, A. (2014). “Strategies to control the high temperature shrinkage of fly ash based geopolymers.” *Thermochimica Acta*, 580, 20-27.

28 Yan S., He P., Jia D., Wang J., Duan X., Yang Z., Wang S., Zhou Y. (2017). “Effects of high-temperature heat treatment on the microstructure and mechanical performance of hybrid C_f-SiC_f-(Al_2O_{3p}) reinforced geopolymer composites.” *Compos. Part B-Eng.*, 114, 289-298

29 Coppola, L., Kara, P., Lorenzi, S. (2016) “Concrete manufactured with crushed asphalt as partial replacement of natural aggregates.”, *Materiales de construcciòn* 66;

30 Coppola, L., Buoso, A., Coffetti, D., Kara, P., Lorenzi, S. (2016) “Electric arc furnace granulated slag for sustainable concrete.” *Construction and Building Materials*, 123, 115-119;

31 Iyer, R. S., Scott, J. A. (2001). “Power station fly ash—a review of value-added utilization outside of the construction industry.” *Resources, Conservation and Recycling*, 31(3), 217-228.

32 Van Beers, D., Bossilkov, A., Lund, C. (2009). “Development of large scale reuses of inorganic by-products in Australia: The case study of Kwinana, Western Australia.” *Resources, Conservation and Recycling*, 53(7), 365-378.

33 Naganathan, S., Razak, H. A., Hamid, S. N. A. (2012). “Properties of controlled low-strength material made using industrial waste incineration bottom ash and quarry dust.” *Materials & Design*, 33, 56-63.

34 Rahman, M. E., Muntohar, A. S., Pakrashi, V., Nagaratnam, B. H., & Sujan, D. (2014). “Self compacting concrete from uncontrolled burning of rice husk and blended fine aggregate.” *Materials & Design*, 55, 410-415.

35 Thomas, M. (2013). “Supplementary cementing materials in concrete.” CRC Press.

36 Swanepoel, J. C., Strydom, C. A. (2002). “Utilisation of fly ash in a geopolymeric material.” *Applied Geochemistry*, 17(8), 1143-1148.

37 Hardjito H., Rangan R.V. (2005). “Development and properties of low-calcium fly ash based geopolymer concrete.” *Research report GC1*. Perth, Australia: Faculty of Engineering, Curtin University of Technology

38 Rashad, A. M. (2014). “A comprehensive overview about the influence of different admixtures and additives on the properties of alkali-activated fly ash.” *Materials & Design*, 53, 1005-1025.

39 Islam, A., Alengaram, U. J., Jumaat, M. Z., & Bashar, I. I. (2014). “The development of compressive strength of ground granulated blast furnace slag-palm oil fuel ash-fly ash based geopolymer mortar.” *Materials & Design*, 56, 833-841.

40 Molino, B., De Vincenzo, A., Ferone, C., Messina, F., Colangelo, F., Cioffi, R. (2014) “Recycling of clay sediments for geopolymer binder production. A new perspective for reservoir management in the framework of Italian Legislation: The Occhito reservoir case study.” *Materials*, 7 (8), 5603-5616.

41 Ferone, C., Liguori, B., Capasso, I., Colangelo, F., Cioffi, R., Cappelletto, E., Di Maggio, R. (2015). “Thermally treated clay sediments as geopolymer source material.” *Applied Clay Science*, 107,

42 Komnitsas, K. (2016). "Co-valorization of marine sediments and construction & demolition wastes through alkali activation." *Journal of Environmental Chemical Engineering*, Volume 4, Issue 4, Part A, 4661–4669.

43 Ferone, C., Colangelo, F., Frattini, D., Roviello, G., Cioffi, R., Di Maggio, R. (2014). “Finite element method modeling of sensible heat thermal energy storage with innovative concretes and comparative analysis with literature benchmarks.” *Energies*, 7(8), 5291-5316.

44 Gil, A., Medrano, M., Martorell, I., Lázaro, A., Dolado, P., Zalba, B., Cabeza, L. F. (2010). “State of the art on high temperature thermal energy storage for power generation. Part 1—Concepts, materials and modellization.” *Renewable and Sustainable Energy Reviews*, 14(1), 31-55.

45 Messina, F., Ferone, C., Colangelo, F., Cioffi R. (2015). “Low temperature alkaline activation of weathered fly ash: influence of mineral admixtures on early age performance.” *Construction and Building Materials*, 86, 169-177

46 Hunter, W. G., Hunter, J. S. (1978). “Statistics for experimenters: an introduction to design, data analysis, and model building (p. 319).” New York: Wiley.

47 Carnì D. L., Scuro C., Lamonaca F., Olivito R.S., Grimaldi D. (2017) “Damage analysis of concrete structures by means of acoustic emissions technique.” *Compos. Part B-Eng.*, 115, 79-86.

48 Rickard, W. D., Kealley, C. S., & Riessen, A. (2015). “Thermally induced microstructural changes in fly ash geopolymers: experimental results and proposed model.” *Journal of the American Ceramic Society*, 98(3), 929-939.

49 Rickard, W. D., Temuujin, J., & van Riessen, A. (2012). “Thermal analysis of geopolymer pastes synthesised from five fly ashes of variable composition.” *Journal of non-crystalline solids*, 358(15), 1830-1839.

50 Ferone, C., Roviello, G., Colangelo, F., Cioffi. R., Tarallo, O. (2013). “Novel Hybrid Organic-Geopolymer materials.” *Appl. Clay Sci.* 73, 42-50.

51 Mishra, S. R., Kumar, S., Park, A., Rho, J., Losby, J., Hoffmeister, B. K. (2003). “Ultrasonic characterization of the curing process of PCC fly ash–cement composites.” *Materials characterization*, 50(4), 317-323.

52 Ohdaira, E., Masuzawa, N. (2000). “Water content and its effect on ultrasound propagation in concrete—the possibility of NDE.” *Ultrasonics*, 38(1), 546-552.

53 Chang, L. S., Chuang, T. H., & Wei, W. J. (2000). “Characterization of alumina ceramics by ultrasonic testing.” *Materials characterization*, 45(3), 221-226.

54 Laux, D., Ferrandis, J. Y., Bentama, J., & Rguiti, M. (2006). “Ultrasonic investigation of ceramic clay membranes.” *Applied Clay Science*, 32(1), 82-86.

55 Palmero, P., Formia, A., Antonaci, P., Brini, S., & Tulliani, J. M. (2015). “Geopolymer technology for application-oriented dense and lightened materials. Elaboration and characterization.” *Ceramics International*, 41(10), 12967-12979.

Captions of the figures

Fig. 1. Objective function (OF) values for the selected mixtures.

Fig. 2. Response of the mean OF to the selected parameters (BA: binder/aggregate ratio; T: treatment temperature; A: additive; t: curing time)

Fig. 3. Mass variation after thermal treatments at different temperatures for mortars number 3, 6 and 9.

Fig. 4. Ultrasonic pulse velocity variations at different curing times for mortars number 3, 6 and 9.

Fig. 5. Ultrasonic pulse velocity variations at different temperature of treatment for mortars number 3, 6 and 9.

Fig. 6. SEM micrographs at 1000X of mortars number 3, 6 and 9 untreated (a, d and g), thermally treated at 150°C (b, e and h) and thermally treated at 550°C (c, f and i)

Table 1. Chemical composition of fly ash and slag (wt%)

	SiO_2	Al_2O_3	Fe_2O_3	CaO	MgO	K_2O	Na_2O	other oxides	SO_3	LOI
FA	53.7	28.1	6.99	4.32	1.59	1.89	0.87	2.54	-	4.53
GGBFS	35.16	10.76	1.40	41.91	7.68	0.14	0.11	0.92	1.92	1.78

Table 2. Factors and levels used in the Design of the Experiment (DOE)

	Binder/aggregate ratio	T Curing (°C)	Additive (% of replaced fly ash)	t curing (hours)
	BA	**T**	**A**	**t**
1	1:2	25	0	24
2	1:2	40	10	48
3	1:2	60	20	168
4	1:1	25	10	168
5	1:1	40	20	24
6	1:1	60	0	48
7	1:0.75	25	20	48
8	1:0.75	40	0	168
9	1:0.75	60	10	24

Table 3. Compressive strength of mortars at room temperature (RT) and variations of physical and mechanical properties after thermal treatment at 150°C

Mixture	Rc (RT) (MPa)	ΔR_c, %	Δm, %	$\Delta \rho$, %
1	9.80 ± 0.80	-14.46	-2.42	-1.23
2	13.27 ± 0.99	-30.4	-1.32	-
3	18.45 ± 0.95	-1.4	-2.71	-0.14
4	8.70 ± 0.30	-25.5	-3.88	-1.37
5	11.55 ± 0.05	-41.0	-3.83	-1.34
6	21.70 ± 0.86	-	-3.38	-1.33
7	8.25 ± 0.05	-3.5	-4.49	-1.35
8	21.00 ±0.99	-25.6	-4.30	-1.83
9	19.33 ± 0.48	-3.5	-4.51	-0.98

Table 4. Variations of mass, density and mechanical strength with treatment temperature

Mixture	**3**				**6**				**9**			
T, °C	**250**	**350**	**450**	**550**	**250**	**350**	**450**	**550**	**250**	**350**	**450**	**550**
Δm, %[a]	3.50	3.89	4.49	5.80	4.46	4.82	6.04	7.96	6.47	7.29	8.24	10.41
Δρ, %[a]	0.86	1.18	2.03	7.67	-	2.45	7.44	10.61	3.49	6.68	7.89	14.59
Rc, MPa	19.14	15.75	17.11	17.66	20.34	17.04	14.98	22.03	18.67	15.59	14.45	11.48
ΔR_c,%[a,b]	-	14.63	7.26	4.28	6.27	21.47	30.97	-	3.41	19.35	25.25	40.61

[a]negative values

[b]values of the loss of mechanical strengths were calculated starting from the mechanical strength of the untreated mortars

Table 5. Thermal conductivity of the experimental mortars

Mortars	Thermal conductivity, (W/m K)
3	0.664±0.0756
6	0.657±0.0260
9	0.745±0.0556

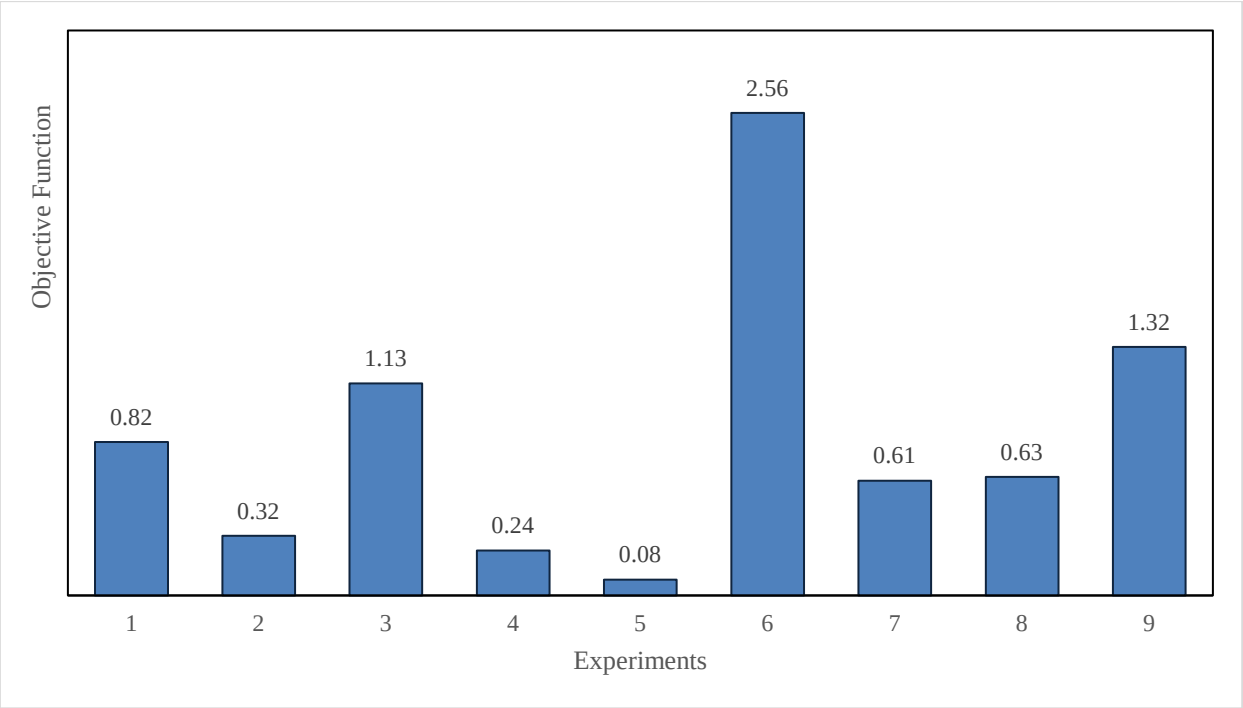
Objective Function
0.82
0.32
1.13
0.24
0.08
2.56
0.61
0.63
1.32
1
2
3
4
5
6
7
8
9
Experiments

Figure 1

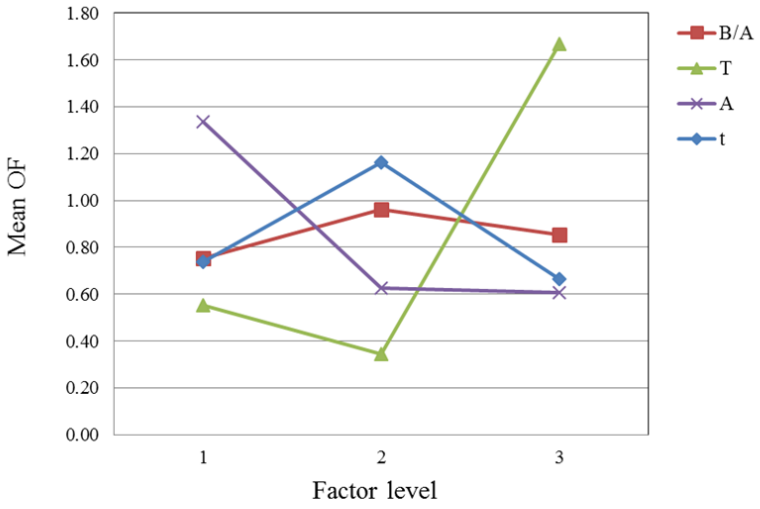
1.80
1.60
1.40
1.20
1.00
0.80
0.60
0.40
0.20
0.00
Mean OF
1
2
3
Factor level
B/A
T
A
t

Figure 2

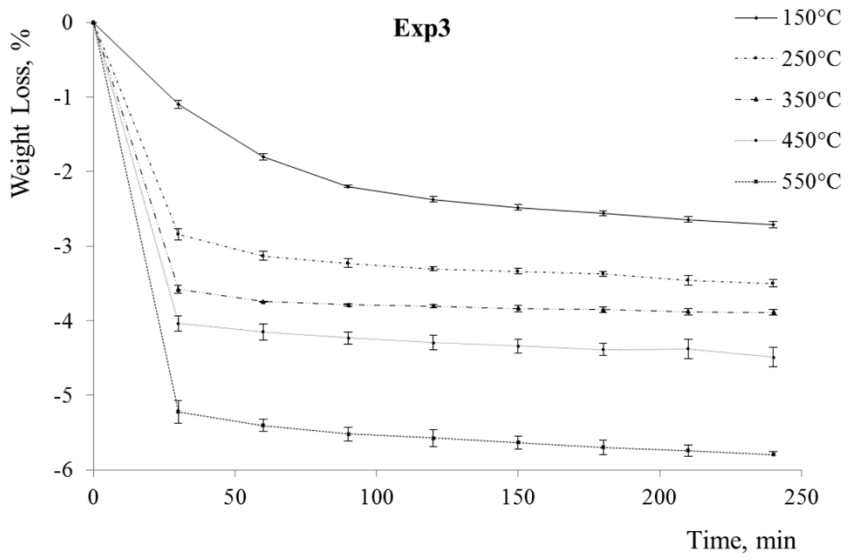
Exp3
150°C
250°C
350°C
450°C
550°C
Weight Loss, %
0
-1
-2
-3
-4
-5
-6
0
50
100
150
200
250
Time, min

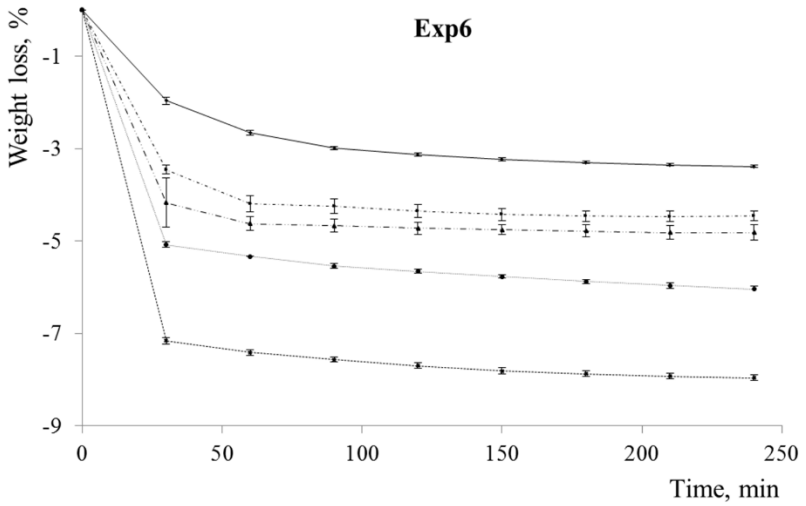
Exp6
Weight loss, %
-1
-3
-5
-7
-9
0
50
100
150
200
250
Time, min

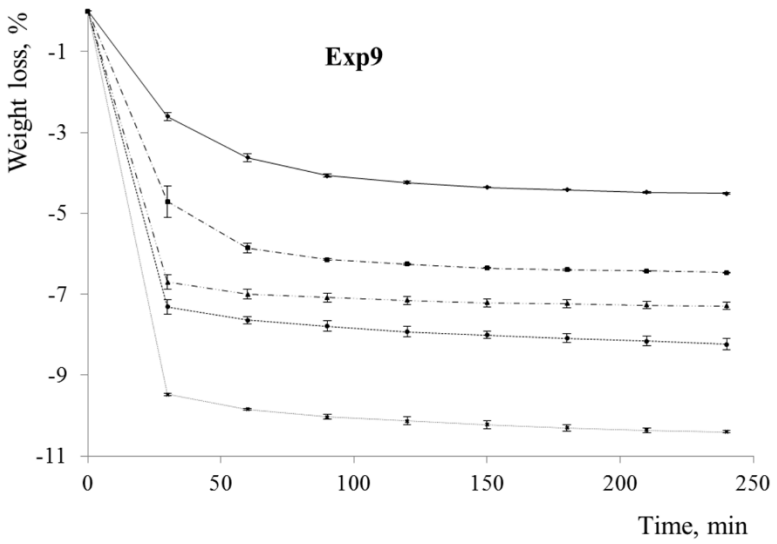
Exp9
Weight loss, %
-1
-3
-5
-7
-9
-11
0
50
100
150
200
250
Time, min

Figure 3

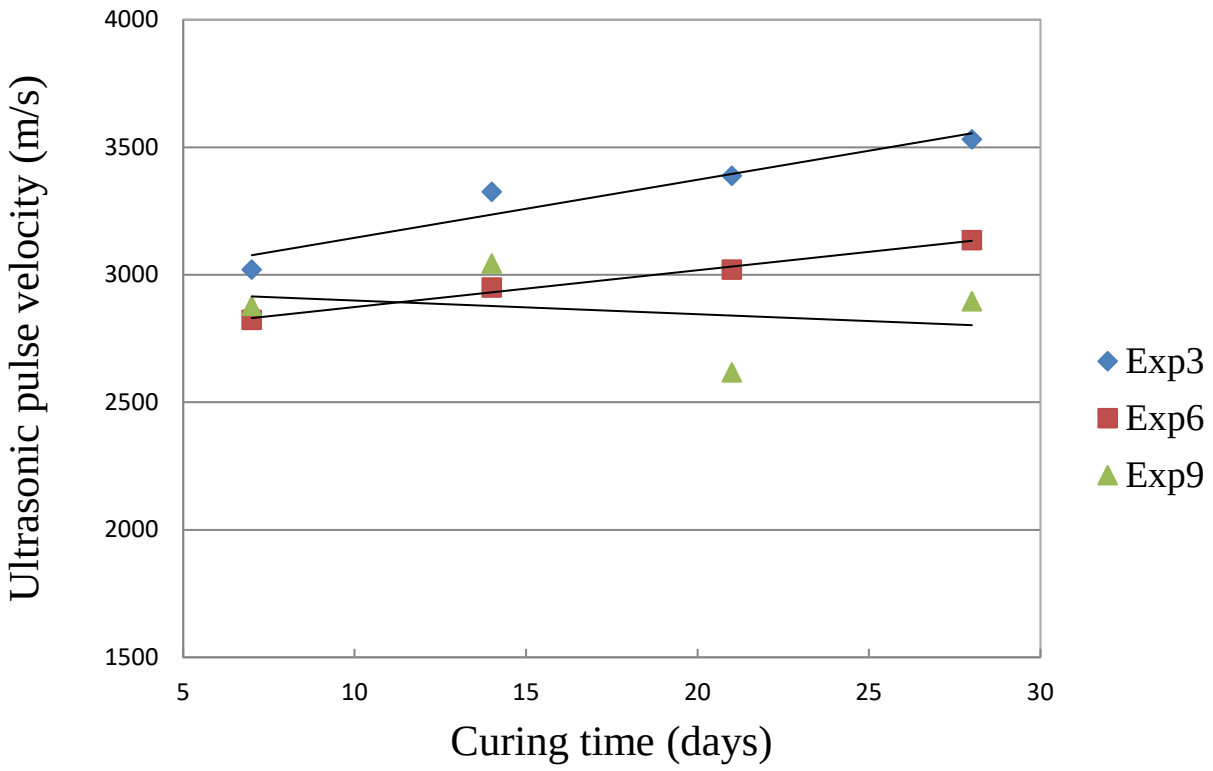
Ultrasonic pulse velocity (m/s)
4000
3500
3000
2500
2000
1500
5
10
15
20
25
30
Curing time (days)
Exp3
Exp6
Exp9

Figure 4

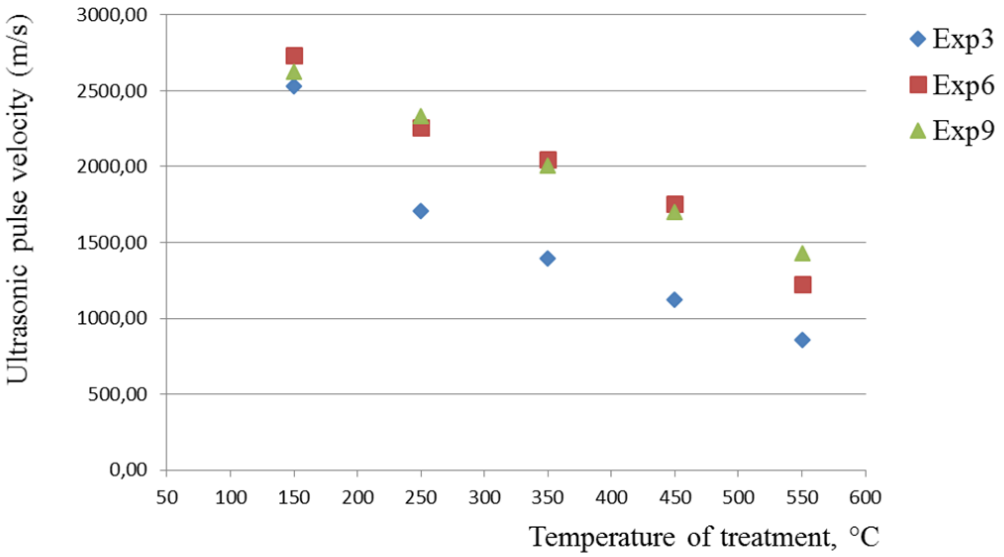
Ultrasonic pulse velocity (m/s)
3000,00
2500,00
2000,00
1500,00
1000,00
500,00
0,00
50
100
150
200
250
300
350
400
450
500
550
600
Temperature of treatment, °C
Exp3
Exp6
Exp9

Figure 5

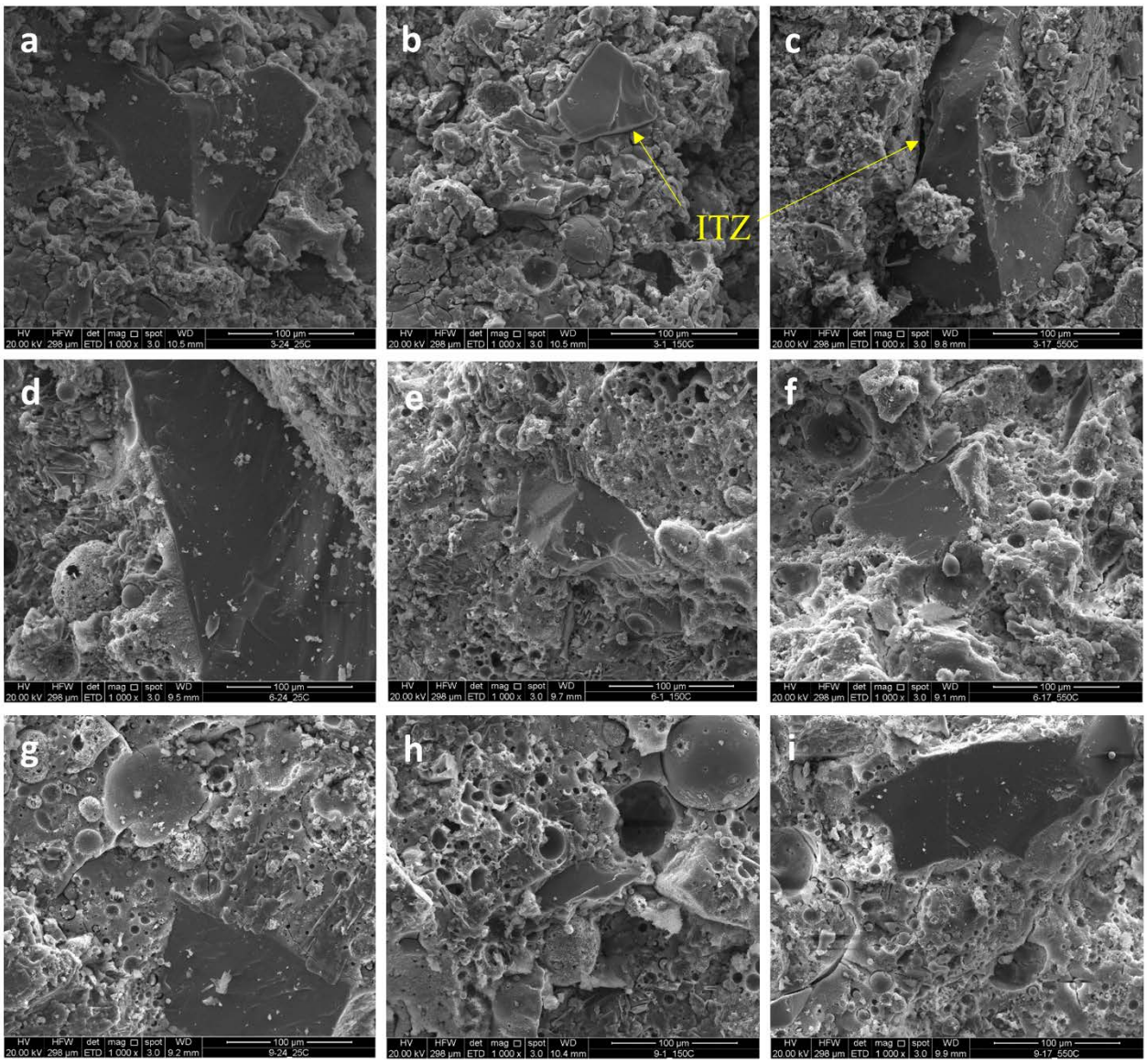

Figure 6